JCTC Journal of Chemical Theory and Computation

ARTICLE

pubs.acs.org/JCTC

The Nature of the Binding of Au, Ag, and Pd to Benzene, Coronene, and Graphene: From Benchmark CCSD(T) Calculations to Plane-Wave DFT Calculations

Jaroslav Granatier,[†,∥] Petr Lazar,[‡,∥] Michal Otyepka,[*,‡] and Pavel Hobza[*,†,‡,§]

[†]Institute of Organic Chemistry and Biochemistry (IOCB), Academy of Sciences of the Czech Republic and Center for Biomolecules and Complex Molecular Systems, Flemingovo nam. 2, 166 10 Prague, Czech Republic

[‡]Department of Physical Chemistry, Faculty of Science, Regional Centre of Advanced Technologies and Materials (RCPTM), Palacky University Olomouc, tr. 17. listopadu 12, 771 46 Olomouc, Czech Republic

[§]Department of Chemistry, Pohang University of Science and Technology (POSTECH), San 31, Hyojadong, Namgu, Pohang 790-784, Korea

ABSTRACT: The adsorption of Ag, Au, and Pd atoms on benzene, coronene, and graphene has been studied using post Hartree−Fock wave function theory (CCSD(T), MP2) and density functional theory (M06-2X, DFT-D3, PBE, vdW-DF) methods. The CCSD(T) benchmark binding energies for benzene−M (M = Pd, Au, Ag) complexes are 19.7, 4.2, and 2.3 kcal/mol, respectively. We found that the nature of binding of the three metals is different: While silver binds predominantly through dispersion interactions, the binding of palladium has a covalent character, and the binding of gold involves a subtle combination of charge transfer and dispersion interactions as well as relativistic effects. We demonstrate that the CCSD(T) benchmark binding energies for benzene−M complexes can be reproduced in plane-wave density functional theory calculations by including a fraction of the exact exchange and a nonempirical van der Waals correction (EE+vdW). Applying the EE+vdW method, we obtained binding energies for the graphene−M (M = Pd, Au, Ag) complexes of 17.4, 5.6, and 4.3 kcal/mol, respectively. The trends in binding energies found for the benzene−M complexes correspond to those in coronene and graphene complexes. DFT methods that use empirical corrections to account for the effects of vdW interactions significantly overestimate binding energies in some of the studied systems.

1. INTRODUCTION

Metals are used as interfaces between graphene and conventional electronics; consequently, it is important to understand the nature of the interactions between metals and graphene if nanoelectronics and nanodevices are to reach their full potential.[1] In addition, nanoparticles of gold and palladium on graphene have found an increasing number of applications as biosensors, highly active catalysts, and energy storage devices.[2−8] Unfortunately, the theoretical description of the interactions between a graphene surface and transition metals is complicated by the large (infinite) number of carbon atoms in the graphene sheet and by the complex electronic structure of the transition metals, which is influenced by relativistic effects and both static and dynamic electron correlation. The size of the systems necessitates the use of periodic boundary conditions (i.e., the description of the electronic structure with a plane-wave basis set). Consequently, studies on the interactions between graphene and transition metals have relied heavily on various plane-wave density functional theory (DFT) methods. Surprisingly, the simple local density approximation (LDA) method still finds widespread use,[9,10] reflecting the fact that this method frequently provides better results (due to cancelation of errors) than fundamentally more accurate generalized gradient approximation (GGA) methods.[11−14] For example, the LDA reproduces the available experimental results for the adsorption of Au on graphite surface better than the other GGA, which underpredicts the strength of binding to Au.[15] However, even the early experiments conducted in the 1970s[16] indicated that the binding of gold on carbon surfaces is heavily dependent on van der Waals (vdW) interactions. This is problematic because neither the LDA nor the various common DFT approaches can describe nonlocal correlation effects, such as vdW interactions. It is worth noting that the physical and chemical nomenclature is not unified; in the physical literature and in this paper, the term "vdW interaction" refers specifically to the London dispersion interaction, which is a weak noncovalent force arising from nonlocal electron correlation. Thus, while the LDA provides a fairly good estimate of the binding energy of gold,[15] it does so for the wrong reason. It is likely that this will have influenced the results obtained in other studies on the adsorption of gold on carbon surfaces,[10,17−19] the adsorption of various metal atoms (including Au, Pd, Fe, and Ti) on graphene,[13] and the adsorption of hydrogen on Pd-decorated graphene.[20] All of these studies were performed using DFT methods that do not account for the contributions of dispersion. It is possible that the adsorption of metals other than gold on carbon surfaces is not governed by the dispersion energy. However, it is impossible to calculate the energy changes involved in the binding of metal atoms to carbon surfaces with thermochemical accuracy (i.e., with errors below 1 kcal/mol) using methods that do not account for dispersion

Received: September 7, 2011
Published: October 05, 2011

energy. Moreover, it is well-known that dispersion energy is an important component of the overall stabilization energy in various types of noncovalent complexes such as those held together by hydrogen bonding, π-stacking, halogen bonding, and other noncovalent interactions.[21] In general, the use of DFT techniques that do not account for dispersion energy causes binding energies to be underestimated.[21]

The aim of the study reported herein was to investigate the interaction of graphene with three different transition metals: gold, silver, and palladium. Since the number of quantum chemical methods that can be used to study infinite graphene sheets is rather limited, we initially studied two smaller systems as models of the graphene surface: benzene and coronene. Because the benzene−M (M = Pd, Au, Ag) complexes are comparatively small, they can be studied using even very accurate and computationally expensive wave function theory (WFT) methods based on the coupled cluster technique with iterative evaluation of the contributions of single and double electron excitations and perturbative evaluation of the contributions of triple excitations (CCSD(T)).[22−24] When used in conjunction with an extended basis set, this method provides stabilization energies for various types of noncovalent complexes with chemical or even higher accuracy (±1 or ±0.1 kcal/mol)[21] and is therefore used to 'benchmark' the performance of less computationally expensive WFT and DFT techniques that account for dispersion interactions in some way. Our first aim was to identify a computational method that is less computationally demanding than CCSD(T) and uses a local basis set but yields good agreement with the CCSD(T) benchmark data. We then planned to use this method to study binding in coronene−M complexes; accurate calculations on these two groups of complexes would provide insights into the nature of the binding of the three different adatoms to carbon surfaces. Specifically, we sought to investigate the performance of the second-order Møller−Plesset (MP2),[25] DFT-D3,[26] and M06-2X[27−29] methods. The DFT-D3 method models the effects of dispersion forces using an additional empirical term that is proportional to R^{-6}, while the M06-2X functional achieves the same objective by incorporating modified parameters into its exchange−correlation functional. Our second aim was to compare the performance of DFT methods utilizing a plane-wave basis set to that of CCSD(T) in the benzene−M model systems. This comparison was performed to identify a DFT method that can be used to accurately model the interactions of transition-metal atoms with graphene. It was anticipated that the results obtained would make it possible to develop general guidelines for the efficient and accurate modeling of extended systems involving vdW interaction.

2. SYSTEMS INVESTIGATED

Benzene−M, coronene−M, and graphene−M (M = Pd, Au, Ag) complexes were investigated. The metal atoms were modeled as being adsorbed at one of three different positions: (t) a 'top' site directly above a C atom, (b) a 'bridge' site above the midpoint of a C−C bond, and (h) the 'hollow' site above the center of the aromatic ring. In the case of coronene, the analogous positions above the central benzenoid ring were considered (Figure 1).

3. CALCULATIONS

Benchmarking calculations on the benzene−M complexes were carried out at the spin-adapted CCSD(T) level with a restricted closed-/open-shell Hartree−Fock (HF) reference function.[22−24,30] Because of the high computational demands of CCSD(T), the MP2 method[25] was also used. The $(n-1)p^6$ $(n-1)d^{10}$ shells of palladium and $(n-1)p^6$ $(n-1)d^{10}$ ns^1 shells of silver and gold were correlated. With the exception of the $1s^2$ electrons of the carbon atoms, all of the electrons in benzene and coronene were correlated.

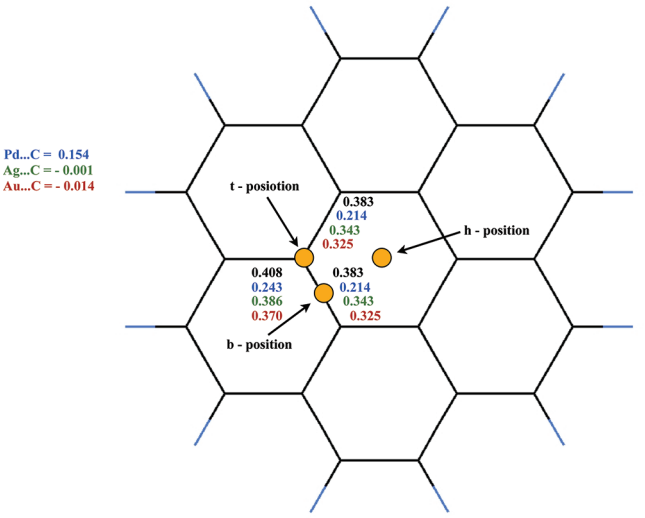

Figure 1. Coronene molecule, showing the three potential sites for the adsorption of metal atoms. Figure also shows the charge distribution in the bonds of the free coronene molecule (black), the coronene−Pd complex (blue), the coronene−Ag complex (green), and the coronene−Au complex (red), as calculated using the M06-2X method. Geometries of the complexes were optimized at the M06-2X level, starting from geometries in which the metal was adsorbed at the (t) position. All final optimized geometries have been bonded on the coronene in (t) position.

Relativistic effects, which are important in heavy transition metals (especially gold) and their complexes,[31] were modeled using the scalar one-component Douglas−Kroll−Hess approximation[32,33] in all wave function methods. All relativistic MP2 and CCSD(T) calculations were performed with ANO-RCC basis sets.[34,35] These basis sets contain diffuse and polarization functions, which are important when studying noncovalent interactions. Another advantage of these basis sets is that they are available with various degrees of contraction. All benchmark CCSD(T) calculations on the benzene−M complexes were performed with the VTZP contraction. MP2 calculations were performed using the VDZP and VTZP contractions as well as with a combination denoted VDZP/VTZP (VDZP for benzene and VTZP for the metal). To compare the relativistic and nonrelativistic CCSD(T) binding energies, calculations were also performed using the relativistic Pol-DK[36] basis sets and the otherwise-equivalent nonrelativistic Pol basis sets,[37] both of which are suitable for calculating molecular electronic properties and the interaction energies of noncovalent complexes.[38] This was done because comparisons of the relativistic and nonrelativistic stabilization energies can provide helpful insights into the nature of the bonding between an aromatic system and a metal atom.[39−41] Throughout this paper, the interaction energy is defined as the difference between the energy of a complex and the sum of the energies of its components; it is negative when the components are attracted to one another. The binding energy is defined as the absolute value of the interaction energy and is

therefore always positive. All calculated WFT interaction energies were corrected for the basis set superposition error (BSSE) using the counterpoise correction.[42] RHF/ROHF, MP2, and CCSD(T) energies were calculated using the MOLCAS 7.2 program package.[43]

The DFT-D3/TPSS/def2-QZVP[26] and M06-2X/lanl2dz[27−29] methods were also used to evaluate the interaction energies of the studied complexes. The DFT-D3 method uses an empirical correction term to describe the dispersion energy, while the M06-2X method accounts for dispersion using a reparameterized exchange−correlation functional. Both of the DFT techniques are substantially less computationally demanding than CCSD(T), making them applicable to large molecular systems.

The structures of benzene and coronene were optimized at the MP2/cc-pVTZ level, and their geometries were assumed to be frozen in all subsequent WFT and DFT calculations, with the exception of the M06-2X calculations on the coronene−M complexes, for which the change in the geometry of the coronene induced by adatom adsorption was studied by full reoptimization of the complex. The DFT-D3 calculations were performed using Turbomole 6.0,[44] and the M06-2X calculations were performed using Gaussian 09.[45]

Plane-wave DFT calculations for an infinite graphene surface were performed using the Vienna Ab initio Simulation Package (VASP) which makes use of the projector augmented wave (PAW) construction for the pseudopotential.[46,47] The GGA of Perdew−Burke−Ernzerhof (PBE)[48] was used to parametrize the exchange−correlation functional. All calculations were carried out using scalar relativistic approximation, i.e., without spin−orbit coupling (except one test calculation for benzene−Au complex, which is discussed later in the text). The structural parameters of benzene and graphene were relaxed by minimizing the forces acting on the atoms using a conjugate gradient algorithm. The energy cutoff for the plane-wave expansion of the eigenfunctions was set to 500 eV. The periodically repeating benzene molecules were separated by at least 8 Å of vacuum in the plane containing the benzene ring and 18 Å of vacuum in the perpendicular direction. The graphene sheet was modeled using a 4×4 supercell, i.e. each supercell contained 32 carbon atoms, using the calculated C−C bond length of 1.44 Å. The repeated sheets were separated from each other by 18 Å of vacuum, and the shortest distance between metal atoms was 10 Å. This construction minimizes electrostatic interactions between repeated images. A Γ-centered $5 \times 5 \times 1$ k-point mesh was found to provide converged total energies and was consequently used for Brillouin zone integration. Spin polarization was taken into account in all calculations. Long range vdW (dispersion) interactions, which are absent in standard DFT, were included by means of the vdW density functional (vdW-DF)[49] for PBE-optimized geometries. The core of the vdW-DF method is a fully nonlocal expression for the correlation energy E_c^{nl}, which takes the following form:

$$E_c^{nl} = \int \mathrm{d}r^3 \mathrm{d}r'^3 n(r) \Phi(r, r') n(r') \quad (1)$$

Here, $n(r)$ is the electron density obtained from a standard DFT calculation and the kernel $\Phi(r, r')$ is a function that depends on $r - r'$ and the magnitudes and gradients of the electron densities at the points r and r'. We used the JuNoLo program to evaluate the vdW term, with PBE electron densities serving as inputs.[50] The vdW-DF method uses standard semilocal GGA functionals to describe the exchange energy. We chose to use the PBE exchange functional, since it was the functional used to calculate the input electron densities. The total energy was then calculated using the expression:

$$E_{tot}^{nl} = E_{tot}^{DFT} - E_c^{PBE} - E_x^{PBE} + (E_x^{PBE} + E_c^{LDA} - E_c^{nl}) \quad (2)$$

We refer to this method as PBE+vdW. The E_x^{PBE} terms are written out explicitly to emphasize the point that the PBE exchange energy inside the parentheses could in principle be replaced by that calculated using some other semilocal formulation; the revised Perdew−Burke−Ernzerhof (revPBE) was suggested in the original formulation of the vdW-DF method by Dion et al.,[49] and other exchange functionals have also been considered.[51,63] In this paper, we propose a different approach; in the spirit of the hybrid screened exchange functionals, we replaced one-quarter of E_x^{PBE} with the exact Hartree−Fock exchange, E_x^{HF}, which was evaluated in VASP using one-electron Kohn−Sham orbitals. The resulting total energy is denoted as EE+vdW. Notice that E_x^{HF} does not match the local density exchange in the constant density limit and so one should not simply exchange E_x^{PBE} for E_x^{HF}. A rationale for mixing one-quarter of E_x^{HF} with the approximate local density exchange was provided by Perdew et al.,[48] who showed that this hybrid matches the LDA in value, slope, and second derivative and is therefore readily embedded into the DFT scheme.

Table 1. DK Relativistic and Nonrelativistic Values of the IP, EA, and Dipole Polarizability (α) for Metal Atoms[a]

	IP (eV)		EA (eV)		α
	DK rel.	nonrel.	DK rel.	nonrel.	DK rel.
Pd (MP2)	8.781		0.248		24.581
Pd (CCSD(T))	8.372		0.521		
Pd (expt)	8.3369[56]		0.5621[57]		
Ag (MP2)	7.615	7.013	1.109	0.880	
Ag (CCSD(T))	7.553	6.990	1.279	1.064	52.46[58]
Ag (expt)	7.57623[59]		1.304481[60]		
Au (MP2)	9.342	7.108	2.248	1.043	
Au (CCSD(T))	9.137	7.072	2.250	1.191	36.06[58]
Au (expt)	9.22553[61]		2.308664[62]		

[a] These calculations were been performed using the aug-cc-pVTZ and aug-cc-pVTZ-DK basis sets.[54,55]

4. RESULTS AND DISCUSSION

4.1. WFT and DFT Calculations on Benzene(Coronene)−M Complexes. *4.1.1. Isolated Systems.* The DK relativistic and nonrelativistic CCSD(T) and MP2 one-electron properties of all three metal atoms are presented in Table 1. Benzene and coronene are electron donors, while the metal atoms are electron acceptors. Because of its electron affinity, Au is a much stronger electron acceptor than Ag and Pd. Relativistic effects significantly increase the electron affinity and the ionization potential of the gold atom and decrease its dipole polarizability; these effects are much smaller in the other metals considered. Consequently, it was expected that charge-transfer stabilization would be most important in the gold complexes. Ag has the greatest polarizability, followed by Au and Pd. Consequently, it was expected that the dispersion interaction would be strongest in the

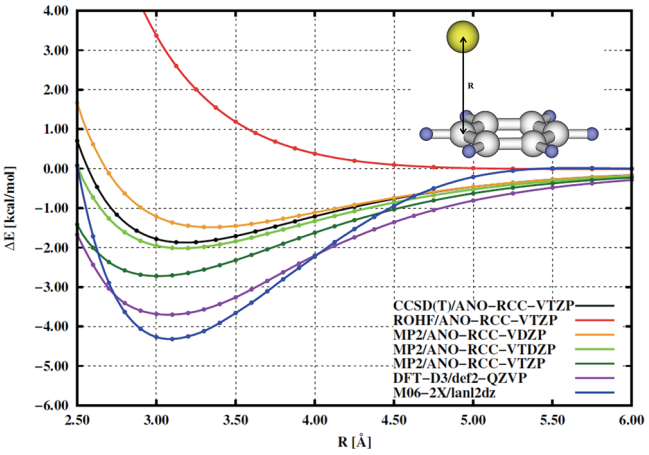

Figure 2. Relativistic WFT (BSSE corrected RHF/ROHF, MP2, and CCSD(T)) and DFT (DFT-D3 and M06-2X) potential energy curves for the benzene−Ag complex with the metal adsorbed at the (t) position.

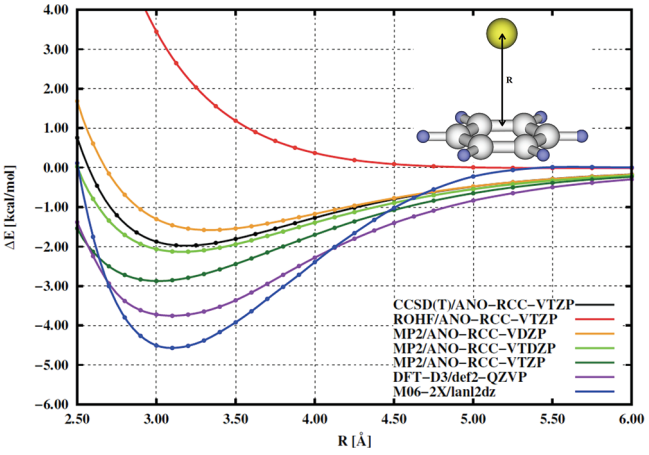

Figure 3. Relativistic WFT (BSSE corrected RHF/ROHF, MP2, and CCSD(T)) and DFT (DFT-D3 and M06-2X) potential energy curves for the benzene−Ag complex with the metal adsorbed at the (b) position.

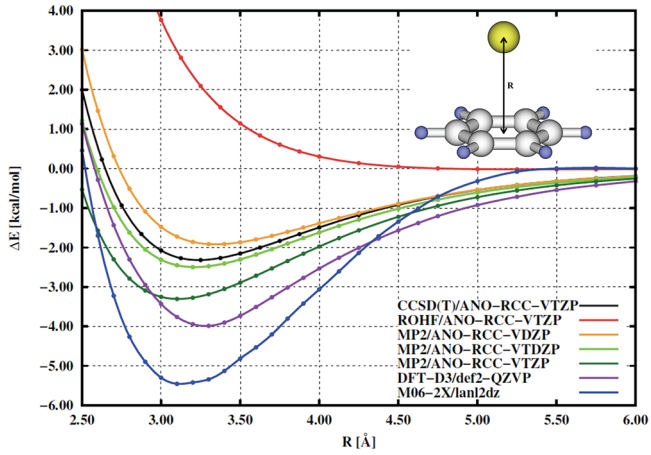

Figure 4. Relativistic WFT (BSSE corrected RHF/ROHF, MP2, and CCSD(T)) and DFT (DFT-D3 and M06-2X) potential energy curves for the benzene−Ag complex with the metal adsorbed at the (h) position.

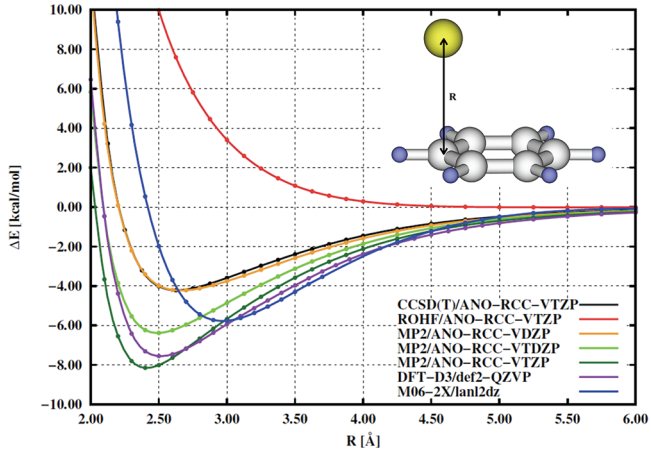

Figure 5. Relativistic WFT (BSSE corrected RHF/ROHF, MP2, and CCSD(T)) and DFT (DFT-D3 and M06-2X) potential energy curves for the benzene−Au complex with the metal adsorbed at the (t) position.

benzene(coronene)−Ag complexes and would become progressively smaller in the corresponding Au and Pd species.

4.1.2. Benzene−M Complexes. Figures 2−10 and Table 2 show the characteristics of all complexes investigated in this work. The benzene−Au complex with the Au atom positioned over a carbon atom (t) was energetically similar but slightly more stable than that in which the metal atom was positioned over a C−C bond (b); both were more stable than that in which the gold atom occupied the 'hollow' site (h) above the center of the ring. The same relative order was given by all methods investigated. The benchmark (DK rel. CCSD(T)/ANO-RCC-VTZP) binding energies for the (t), (b), and (h) positions were 4.2, 4.1, and 3.2 kcal/mol, respectively. The DK-MP2/ANO-RCC-VDZP method yielded similar binding energies to CCSD(T) for all positions, but MP2 calculations using the larger VTDZP and VTZP basis sets (cf. Figures 5−7) overestimated the binding energies. M06-2X and DFT-D3 systematically overestimated the binding energies by 40−100%. For the (t) and (b) positions, the DFT-D3 energies were in worse agreement with the benchmark data than those obtained with M06-2X, but M06-2X strongly overestimates the stabilization for the (h) position. The M06-2X results were also qualitatively inconsistent with the CCSD(T) benchmarks in that they predict the complex with the gold atom in the (h) site to be the most stable.

The situation changes somewhat on switching from Au to Ag. Specifically, the calculated CCSD(T) energies for all three Ag adsorption positions were similar; the species generated by adsorption above the 'hollow' (h) was the most favorable but was only 25% more stable than the least favorable, which was generated by adsorption over a carbon atom (t). Similar trends were observed with all of the computational methods examined. The benchmark binding energies for the (h), (b) and (t) positions (2.3, 2.0, and 1.9 kcal/mol, respectively) are smaller than the corresponding values for the benzene−Au complexes by about 30% for (h) and 50% for the (t) and (b) positions. Additionally, the equilibrium distances between the metal atom and the ring were more than 0.5 Å larger in the Ag species than in their Au counterparts for the (b) and (t) positions. As was the case with the Au species, DK-MP2/ANO-RCC-VDZP provided binding energies that mirrored the benchmark results fairly

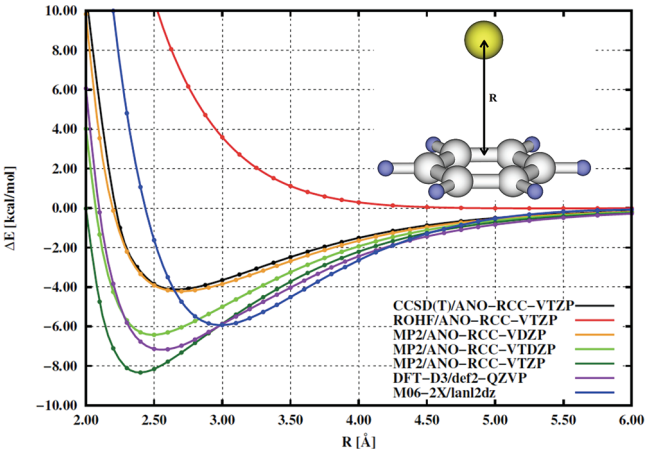

Figure 6. Relativistic WFT (BSSE corrected RHF/ROHF, MP2, and CCSD(T)) and DFT (DFT-D3 and M06-2X) potential energy curves for the benzene−Au complex with the metal adsorbed at the (b) position.

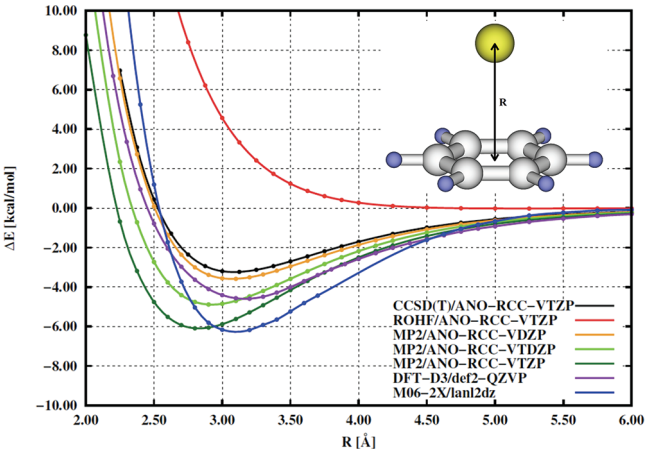

Figure 7. Relativistic WFT (BSSE corrected RHF/ROHF, MP2, and CCSD(T)) and DFT (DFT-D3 and M06-2X) potential energy curves for the benzene−Au complex with the metal adsorbed at the (h) position.

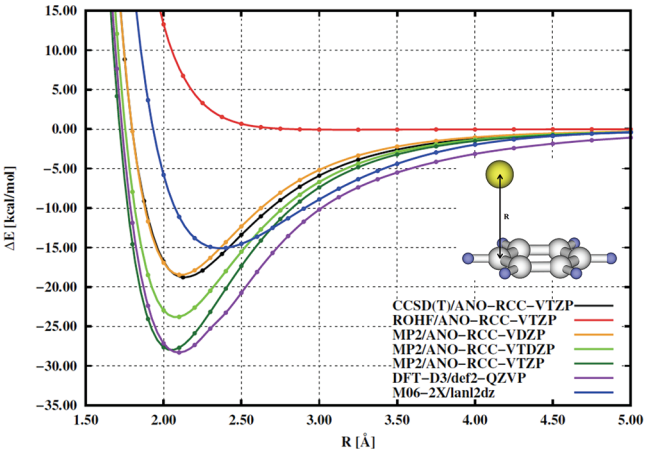

Figure 8. Relativistic WFT (BSSE-corrected RHF/ROHF, MP2, and CCSD(T)) and DFT (DFT-D3 and M06-2X) potential energy curves for the benzene−Pd complex with the metal adsorbed at the (t) position.

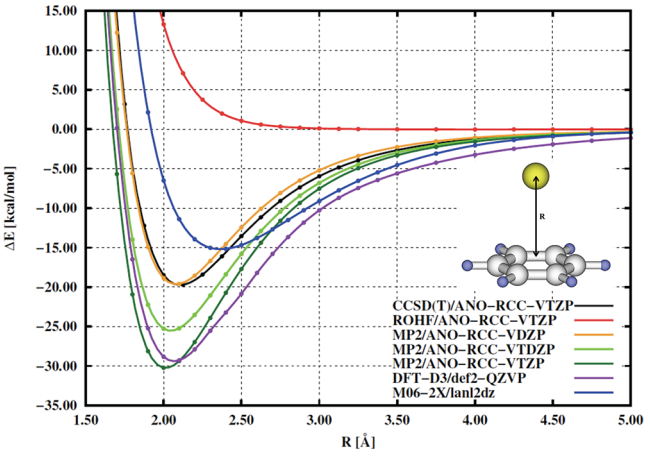

Figure 9. Relativistic WFT (BSSE-corrected RHF/ROHF, MP2, and CCSD(T)) and DFT (DFT-D3 and M06-2X) potential energy curves for the benzene−Pd complex with the metal adsorbed at the (b) position.

closely, while MP2 with triple-ζ basis set overestimated the binding energies (cf. Figures 2−4). Neither of the DFT methods examined provided reliable binding energies; both DFT-D3 and M06-2X strongly overestimated the stabilization for all three positions.

The low binding energies for Au and Ag are indicative of noncovalent binding. The binding energies for Pd were an order of magnitude higher, suggesting that in this case, the interaction between the metal and the arene is partially covalent. The (b) and (t) positions, which are similar in energy, are preferred to (h), and all methods examined yielded the same order of energies. The benchmark binding energies for the (b), (t), and (h) positions were 19.7, 18.8, and 12.8 kcal/mol, respectively. These higher binding energies were associated with considerably shorter internuclear distances between the Pd and C atoms than was the case in the Au and Ag complexes; adsorption of Pd in the (t) position resulted in an internuclear distance of only 2.1 Å, which is similar to the length of covalent C−Pd bonds. As in both of the preceding cases, DK-MP2/ANO-RCC-VDZP was the method whose energies were in best agreement with the benchmark values, with the other MP2 methods once again significantly overestimating the binding energies for all three positions (cf. Figures 8−10). DFT-D3 also significantly overestimates the binding energies (by 35% or more), but M06-2X provides binding energies that agree quite well with the benchmark values, although the (t) and (b) sites are slightly underbound.

These results clearly demonstrate that the interactions of Pd atoms with benzene differ significantly from those of Au and Ag atoms. The binding energies of Pd are much higher than those of Au and Ag, and the corresponding internuclear distances are much shorter. The Au and Ag binding energies are in the range typically associated with noncovalent interactions, whereas the Pd binding energies encroach on ranges more commonly associated with covalent bonds. All three binding sites yield broadly similar binding energies for the adsorption of Au and Ag, but the (b) and (t) positions are clearly favored over the (h) site in the case of Pd adsorption. Of the computational methods tested, DK-MP2/ANO-RCC-VDZP provided the best

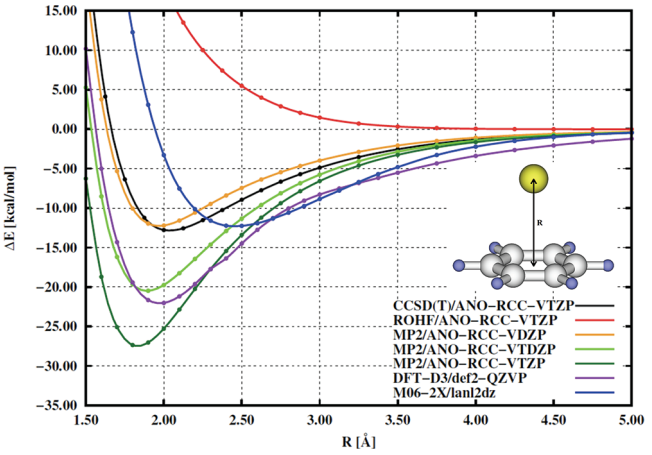

Figure 10. Relativistic WFT (BSSE-corrected RHF/ROHF, MP2, and CCSD(T)) and DFT (DFT-D3 and M06-2X) potential energy curves for the benzene−Pd complex with the metal adsorbed at the (h) position.

agreement with the benchmark CCSD(T) energies and can thus reasonably be expected to provide accurate results when applied to larger model systems. It should be noted that better agreement for double-ζ basis set (than for triple-ζ basis set) arises from compensation of errors. However, while the MP2 method is less expensive than CCSD(T), it is still rather computationally demanding. Of the faster DFT techniques, M06-2X is preferable to DFT-D3, since it gave absolute binding energies that better matched the benchmark values. However, when considering the relative magnitudes of the binding energies for the three elements, a different picture emerges. The CCSD(T) benchmark calculations indicate that the binding energy of Pd to benzene is nine times greater than that of Ag and that of Au is two times greater, giving a benchmark Pd:Au:Ag ratio of 9:2:1. The MP2 (10:2:1) and DFT-D3 ratios (7:2:1) matched the benchmark values fairly closely, but the M06-2X results (3:1:1) strongly disfavor Pd. Thus, for comparing the binding energies of different metals, MP2 and DFT-D3 appear to be superior to M06-2X.

Our results strongly contradict the findings of previous studies in which DFT methods were used. For example, DFT/BPW91/TZP calculations[52] on benzene−M (M = Ag and Au) complexes provided binding energies for the (h), (b) and (t) positions of 5.7, 5.3, and 5.3 kcal/mol, respectively, for Ag, and 5.3, 5.1, and 3.9 kcal/mol, respectively, for Au. These findings are clearly incompatible with the benchmark data reported herein, since they suggest that the binding energies for Au are smaller than those for Ag. This is probably due to the neglect of relativistic effects at the DFT/BPW91/TZP level of theory; relativistic effects change the nature of binding in the benzene−Au complexes, as discussed below.

4.1.3. Nature of the Bonding in Benzene−M Complexes. The nature of the metal−arene binding in all three complexes differs, as indicated by the differences in the binding energies calculated using different levels of theory. The omission of the correlation energy causes the binding energies to be strongly underestimated. Figures 2−10 show that the HF energy curves for all atoms and all adsorption positions are universally repulsive, i.e., no binding occurs. This indicates that the stabilization of all benzene−M complexes originates from correlation effects. However, while correlation effects are important in the binding of all three of the investigated metals, relativistic effects are only important in the Au complexes. This conclusion is supported by the calculated one-electron properties shown in Table 1. The calculated ionization potential and electron affinity of Au change dramatically when relativistic effects are included; these in turn affect the benzene−Au binding energies, which are significantly reduced by the omission of relativistic effects. The relativistic CCSD(T)/Pol-DK binding energies are 3.7, 3.7, and 3.1 kcal/mol for the (t), (b), and (h) positions, respectively; the corresponding nonrelativistic binding energies are significantly smaller (2.0, 2.1, and 2.5 kcal/mol, respectively). For the sake of comparison, we also determined the relativistic vs nonrelativistic binding energies for the (t), (b), and (h) positions of the benzene−Ag complex, which were 2.1, 2.2, and 2.6 vs 1.9, 2.0, and 2.4 kcal/mol, respectively.

One of the most reliable ways of obtaining information on the nature of the bonding is to compare the electronic structure of the bound species to that of the isolated atom. In the case of Ag, such comparisons indicate that the stabilization of the benzene−Ag complex is almost entirely due to the London dispersion energy. This is consistent with the high polarizability of Ag and the relatively large distance between the Ag nucleus and the benzene ring, which means that there is very little overlap of the orbitals of the metal and the arene. Indeed, the orbitals of the complex are almost identical to those of its separated constituents. Analysis of the charge transfer in the Ag complexes (Mulliken charges, determined using the MP2/ANO-RCC-VDZP method) revealed that Ag carries a negative charge of −0.05 e in all of the structures examined, i.e., it acts as an electron acceptor, while benzene is an electron donor. Because of the low electron affinity of Ag and the large separation of the metal atom and the arene, there is relatively little charge transfer from benzene to the Ag atom.

Compared to Ag, Au is significantly less polarizable and has a higher electron affinity (Table 1). The lower polarizability of Au implies that dispersion interactions will be less important in its complexes, and the higher electron affinity is likely to increase the importance of charge-transfer interactions. Mulliken population analyses indicated that the magnitude of the charge transfer in the benzene−Au complexes was approximately twice that in the benzene−Ag complexes, with the Au atom carrying negative charges of −0.11 and −0.12 e for the (t) and (b) positions, respectively. This enhanced charge transfer is attributable to relativistic effects because their omission halves the electron affinity of the gold atom (Table 1). The stabilization of the benzene−Au complex by charge-transfer interactions is demonstrated by the fact that their binding energies are more than twice as large as those for the corresponding benzene−Ag complexes and by the considerably shorter (by more than 0.5 Å) distances between the benzene ring and the metal atom in the gold complexes. These shorter distances reflect a greater overlap between the orbitals of the two systems. Specifically, the formation of new bonding and antibonding orbitals from the doubly occupied $5d_0$ orbital of Au and the benzene p_z orbitals was observed. This interaction model, which highlights the importance of charge transfer, has been presented in previous works.[39−41] The dramatic increase in stability for complexes of Au is due to relativistic effects, which increase the metal's electron affinity and thus favor the transfer of charge from the ligand to the metal. While charge transfer plays a key role for gold atoms in the (b) and (t) positions, it is less pronounced in the (h) position; here, the dispersion energy provides a larger contribution to the binding energy. It is worth noting that for Au^+ and Ag^+ ion−arene complexes, the bonding becomes mainly electrostatic, and binding energies are almost an order of magnitude higher.[64−66]

Table 2. Extrapolated Interaction Energies ΔE [kcal/mol] and Optimal Bond Lengths R (in terms of the shortest distance between the metal atom and the benzene plane) [Å] for Benzene−M (M = Ag, Au, Pd) Complexes Calculated at the Various DFT with Dispersion Correction and DK Relativistic and Nonrelativistic WFT Levels

	benzene−Pd			benzene−Ag			benzene−Au		
	(t)	(b)	(h)	(t)	(b)	(h)	(t)	(b)	(h)
				DFT-D3/TPSS/def2-QZVP					
ΔE	−28.3	−29.4	−22.1	−3.7	−3.7	−4.0	−7.5	−7.2	−4.6
R	2.10	2.07	1.97	3.07	3.10	3.28	2.51	2.56	3.17
				M06-2X/lanl2dz					
ΔE	−15.1	−15.2	−12.3	−4.3	−4.6	−5.5	−5.8	−5.9	−6.3
R	2.36	2.37	2.45	3.09	3.10	3.12	2.97	2.99	3.10
				DK rel. MP2/ANO-RCC-VDZP					
ΔE	−18.5	−19.6	−12.3	−1.5	−1.6	−1.9	−4.2	−4.2	−3.6
R	2.11	2.08	1.97	3.34	3.33	3.34	2.66	2.69	3.07
				DK rel. MP2/ANO-RCC-VTZP					
ΔE	−28.0	−30.2	−27.5	−2.7	−2.9	−3.3	−8.1	−8.3	−6.1
R	2.05	2.01	1.83	3.01	3.01	3.11	2.41	2.39	2.83
				DK rel. CCSD(T)/ANO-RCC-VTZP					
ΔE	−18.8	−19.7	−12.8	−1.9	−2.0	−2.3	−4.2	−4.1	−3.2
R	2.13	2.11	2.04	3.18	3.18	3.24	2.63	2.67	3.09
				DK rel. CCSD(T)/Pol-DK					
ΔE	–	–	–	−2.1	−2.2	−2.6	−3.7	−3.7	−3.1
R	–	–	–	3.19	3.19	3.24	2.73	2.79	3.17
				nonrel. CCSD(T)/Pol					
ΔE	–	–	–	−1.9	−2.0	−2.4	−2.0	−2.1	−2.5
R	–	–	–	3.29	3.29	3.29	3.36	3.37	3.39
				GGA PBE					
ΔE	−26.3	−27.3	−19.0	−1.3	−1.2	−1.0	−6.1	−5.6	−1.63
R	2.10	2.07	2.01	3.05	3.10	3.39	2.44	2.46	3.09
				PBE+vdW					
ΔE	−21.5	−21.8	−13.3	−2.7	−2.7	−2.6	−5.9	−5.5	−3.6
R	2.17	2.18	2.16	3.17	3.23	3.41	2.70	2.79	3.21
				EE+vdW					
ΔE	−17.2	−18.7	−10.6	−2.4	−2.3	−2.5	−5.1[a]	−4.8	−3.4
R	2.18	2.15	2.16	3.22	3.32	3.41	2.64	2.74	3.22

[a] EE + vdW + spin−orbit coupling (soc) −5.7 kcal/mol.

The metal−ligand bonding in the benzene−Pd complexes differs significantly from that in the Ag and Au complexes due to the different electronic structure of Pd. In the ground state, the valence d-orbitals of palladium are fully occupied, and the first virtual orbital is the 5s. In all of the benzene−Pd complexes examined in this work, the Pd atom carried a small positive charge, indicating that it was acting as an electron donor. Detailed analyses indicated a significant loss of electron density from the Pd valence d-orbitals (relative to the situation in the free atom) and a simultaneous significant increase in electron density in the virtual 5s orbital. This is consistent with the formation of a so-called dative bond, in which charge is transferred from Pd to benzene, leading to an increase in the electron density of the benzene ring and a decrease in that of the Pd atom. This polar complex is then stabilized by back donation of charge from the carbon atom to the valence 5s orbital of Pd. A dative bond of this kind would account for the high binding energies observed for the benzene−Pd complex.

4.1.4. Coronene−X Complexes. Coronene is a more complex model of graphene than benzene. The central aromatic ring of coronene (Figure 1) is surrounded only by other aromatic rings, and all its carbon atoms bind exclusively to other carbon atoms. We investigated the binding of Ag, Au, and Pd atoms to coronene using the MP2/ANO-RCC-VDZP, DFT-D3/def2-QZVP, and M06-2X/lanl2dz methods, as discussed in the preceding section. The size of the coronene complexes meant that it would have been impractical to perform CCSD(T) calculations on them to obtain benchmark binding energies. Therefore, binding energies calculated using the MP2 method were used as reference values for the coronene complex, since this level of theory provided absolute and relative binding energies that were reasonably close to the benchmark CCSD(T) values for all of the benzene−metal

Table 3. DK rel. MP2, DFT-D3, and M06-2X Extrapolated Interaction Energies ΔE [kcal/mol] and Metal Atom Charges [e] for Coronene−M (M = Ag, Au, Pd) Complexes with an Optimized Bond Length R [Å]

	coronene−Pd			coronene−Ag			coronene−Au		
	(t)	(b)	(h)	(t)	(b)	(h)	(t)	(b)	(h)
				MP2					
ΔE	−17.7	−17.9	−13.7	−3.9	−4.0	−4.1	−6.9	−7.0	−6.7
R	2.11	2.09	1.99	∼3.17	∼3.13	∼3.19	2.83	2.82	2.92
charge	0.051	0.045	0.032	−0.052	−0.052	−0.051	−0.068	−0.067	−0.063
				DFT-D3					
ΔE	−26.3	−26.9	−24.6	−5.7	−5.8	−6.0	−7.3	−7.3	−6.7
R	2.12	2.08	1.99	3.16	3.14	3.21	2.80	2.84	3.09
				M06-2X					
ΔE	−14.0	−14.1	−12.8	−6.3	−6.3	−6.0	−7.2	−7.2	−7.0
R	2.46	2.45	2.47	3.12	3.12	3.12	3.06	3.06	3.09
charge	0.073	0.075	0.067	−0.010	−0.009	−0.007	−0.028	−0.027	−0.027

complexes discussed in the preceding section. The M06-2X method was used to optimize the geometries of the coronene−M complexes and to estimate the changes in the electronic structure of the coronene following adatom adsorption.

The MP2, DFT-D3, and M06-2X binding energies and equilibrium distances for all of the coronene complexes considered are summarized in Table 3. It is apparent that the binding energies for the coronene complexes differ from their benzene counterparts. At the MP2 level, it was found that the binding energies for Au and Ag increased on going from benzene to coronene, by around 50% in the case of Au and around 100% in the case of Ag. Conversely, going from benzene to coronene reduced the binding energy of Pd by around 10%, although binding in the (h) position was slightly stronger in the coronene complex than in the corresponding benzene species. However, the relative strength of binding to Pd, Au, and Ag remained as it had been in the case of benzene, as did the relative binding energies for adsorption at different positions around the ring. For the Au complexes, the internuclear distances between the metal and the plane containing the arene increased on going from benzene to coronene; for the Ag complexes, the corresponding internuclear distances decreased. However, in both cases, the differences between the distances in the benzene and coronene complexes were small. No significant difference in distance was observed in the Pd complexes. It appears that the nature of the metal−arene bond in the coronene−Pd complexes is very similar to that in the benzene−Pd complexes; a "covalent" bond is formed between the carbon atoms and Pd by the overlap of the d-orbitals of Pd with the π orbitals of the coronene. Silver atoms bind exclusively via dispersion forces; while the polarizability of coronene is greater than that of benzene, this is outweighed by the fact that the coronene complexes have a greater number of carbon atoms and therefore experience more exchange repulsion than their benzene counterparts. This is the cause of the greater carbon−Ag distances in coronene complexes of silver. The situation with the gold complexes is more complicated, because both the dispersion energy and the charge transfer are important in their stabilization. As with the Ag complexes, the exchange repulsion is greater in the coronene complexes of Au than in the benzene species, and so the distances between the Au atom and the plane containing the arene are somewhat greater in the coronene complexes, although the difference is relatively modest. As with the benzene complexes, it is possible to obtain insights into the bonding and charge transfer in coronene−metal complexes by analyzing the Mulliken charges on the adatoms. Both gold and silver atoms in the coronene complexes carry partial negative charges, indicating that both function as electron acceptors. The MP2 charges, which were used as reference values, were greater than the M06-2X charges and can be compared to those calculated for the benzene complexes. While the extent of charge transfer in the silver complexes of benzene and coronene was very similar, the magnitude of the charge transfer in the coronene−Au complexes was approximately 40% smaller than that in the corresponding benzene complexes.

Both the DFT-D3 and M06-2X calculations exhibited trends similar to those observed in the MP2 data, and the relative stabilities of all of the coronene−metal complexes considered were well reproduced. The DFT-D3 interaction energies for the gold complexes were very similar close to those obtained at the MP2 level. However, the DFT-D3 binding energies for the Ag and Pd complexes exceeded the MP2 values by 50% or more. The M06-2X binding energies for the Pd and Au complexes agreed well with the MP2 values, but those for the Ag complex were overestimated by about 60%.

All three methods considered (i.e., MP2, DFT-D3, and M06-2X) indicate that the adsorption of Pd is significantly more favorable than that of Au or Ag, but the extent to which this is the case depends on the method used (MP2, 4:2:1; DFT-D3, 4:1:1; M06-2X, 2:1:1). In all cases, however, the difference between the binding energies for Pd and Ag was smaller than that observed with the corresponding benzene complexes.

Figure 1 shows the (t), (b), and (h) positions for adsorption on coronene and also the M06-2X overlap populations in the C−C bonds that are affected by adsorption. In the case of adsorption of an Ag adatom, there is no significant change in the overlap populations relative to those in the isolated coronene, and the total overlap between Ag and the nearest C is also negligible (−0.001). This is not the case in the corresponding Au complexes, in which all the C−C bonds in coronene are weakened relative to those in the isolated molecule (having electron populations of 0.325, 0.325, and 0.370), but the overlap population of the Au−C bond remains negative (−0.014).

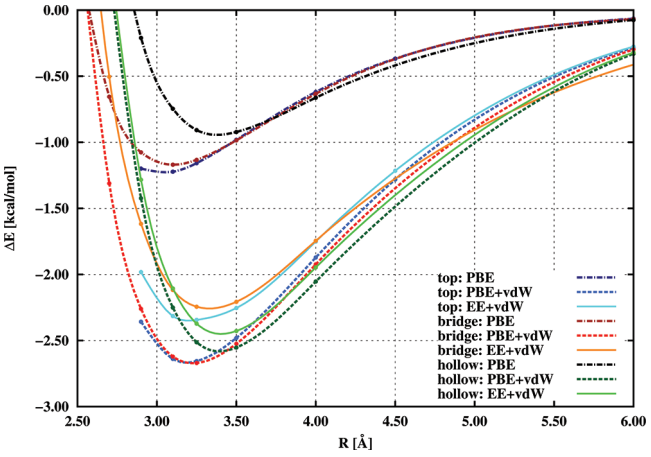

Figure 11. Periodic plane-wave DFT/PBE, DFT/PBE+vdW, and DFT/EE + vdW potential curves for the benzene−Ag complex with the metal adsorbed at the (t), (b), and (h) positions.

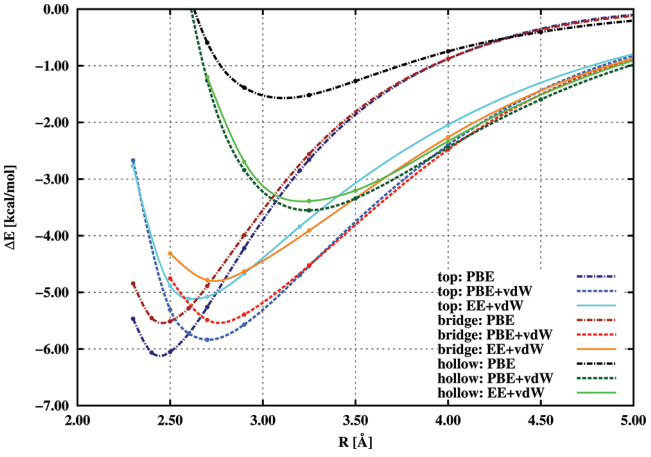

Figure 12. Periodic plane-wave DFT/PBE, DFT/PBE+vdW, and DFT/EE+vdW potential curves for the benzene−Au complex with the metal adsorbed at the (t), (b), and (h) positions.

The C−C bonds in coronene are weakened due to their relatively strong interaction with the Au adatom. Even more dramatic changes occur upon the adsorption of Pd. The Pd−C bond is significantly populated (0.154), and the overlap populations of the C−C bonds are significantly reduced (0.214, 0.214 and 0.243) relative to those in the free coronene. These numbers clearly show that the binding of Ag to coronene (and to some extent, also that of Au) is noncovalent, occurring primarily via dispersion forces, whereas Pd binds covalently. The overlap populations between the Pd and C atoms are comparable to those between carbon atoms in the vicinity of the adsorption site, demonstrating that the adsorption of Pd significantly weakens the covalent C−C bonds in the vicinity of the site of adsorption and results in the formation of a partly covalent bond between the Pd and C atoms.

4.2. Periodic Plane-Wave DFT Calculations. *4.2.1. Benzene−M Complexes.* Figures 11−13 and Table 2 show the binding energies calculated using the plane-wave approach. The main differences between the investigated elements can be seen even in the results of the simple PBE/GGA calculations, although this method is rather unsatisfactory in quantitative terms. Compared to the CCSD(T) benchmark results, the benzene−Pd

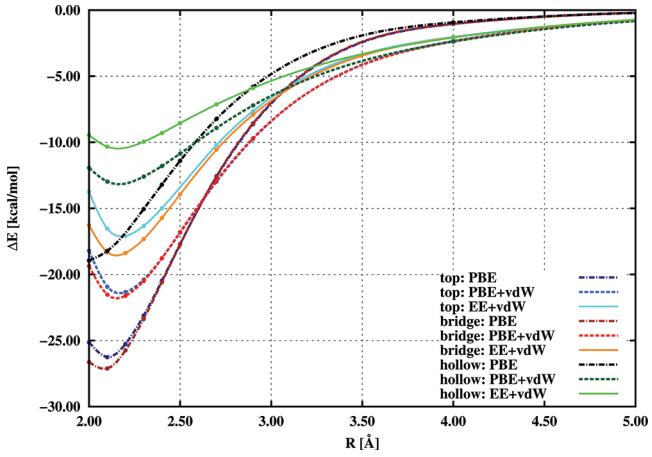

Figure 13. Periodic plane-wave DFT/PBE, DFT/PBE+vdW, and DFT/EE+vdW potential curves for the benzene−Pd complex with the metal adsorbed at the (t), (b), and (h) positions.

and −Au complexes are significantly overbound, whereas the benzene−Ag complex is underbound. On examining the PBE+vdW energy curves, it is apparent that this disagreement is primarily due to the neglect of dispersion forces. The inclusion of dispersion forces affords greatly improved agreement with the benchmark values, as discussed in more detail below. It should be noted that the LDA approximation, which is also used in studies of adsorption on graphene, overestimates the binding energy by more than 100% in all cases examined (data not shown) and yields unreasonably short bond distances as well.

The benzene−Au complex has a total spin moment of 1 μ_B due to the single valence electron of the Au atom. The spin moment does not change substantially as a function of the distance between the Au atom and the benzene ring, indicating that there is negligible charge transfer between the Au atom and the C atoms of the benzene ring. As suggested by the WFT methods, the (t) position is preferred to the (b) position, although the binding energies for these two spots are very similar and are both significantly greater than that for the hollow (h) position. The relative order of energies is the same for all methods investigated, but the calculated energetic differences are reduced when the nonlocal vdW term is incorporated into the calculations. Inspection of the interaction energy curves in Figure 12 indicates that the vdW term is actually repulsive, i.e., the PBE+vdW equilibrium energies and distances are higher than those given by the PBE calculation. The inclusion of one-quarter of exact exchange in the calculation further reduces the binding energies and yields the best agreement with the benchmark CCSD(T) calculations. The EE+vdW binding energies for the (t), (b), and (h) positions are 5.1, 4.8, and 3.4 kcal/mol, respectively. This means that both the values of binding energies and the differences between the binding energies for the (t), (b), and (h) positions are within 1 kcal of the benchmark CCSD(T) values. As gold is known to display significant relativistic effects, we tested the influence of spin−orbit coupling (soc) on the interaction energy for the (t) position. It was found that soc has a slight effect on the total PBE energy but has little impact on the charge density distribution within the complex, which determines the nonlocal vdW contribution (see eq 1). The binding energy for Au in the (t) position as calculated using the EE+vdW+soc method is 5.7 kcal/mol.

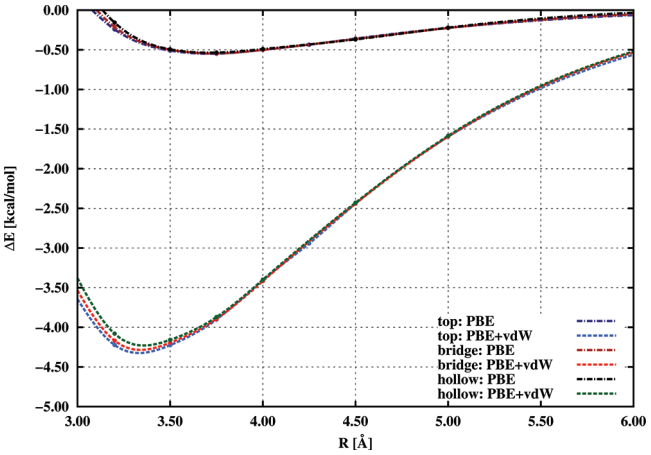

Figure 14. Periodic plane-wave DFT/PBE and DFT/PBE+vdW potential curves for the graphene−Ag complex with the metal adsorbed at the (t), (b), and (h) positions.

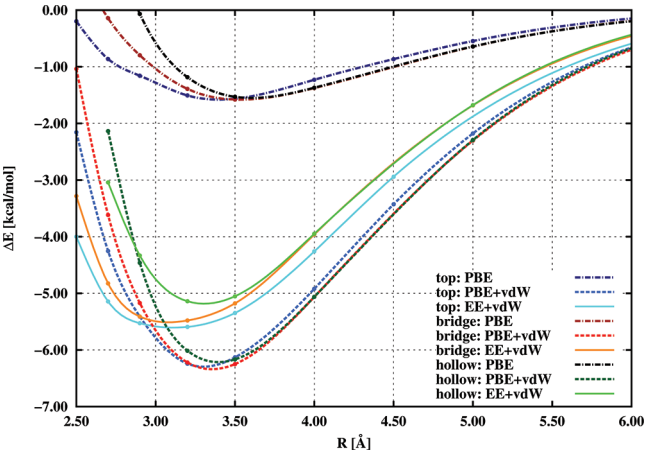

Figure 15. Periodic plane-wave DFT/PBE, DFT/PBE+vdW, and DFT/EE+vdW potential curves for the graphene−Au complex with the metal adsorbed at the (t), (b), and (h) positions.

The potential curves for the benzene−Ag complex are shown in Figure 11 and clearly illustrate the importance of the vdW dispersion term. Using PBE alone, the calculated binding energies for the (t), (b), and (h) positions were 1.3, 1.2, and 1.0 kcal/mol, respectively. Obviously, these values are unrealistically low, especially for the hollow position, which was found to be the preferred site in the CCSD(T) calculations. By including the vdW term, identical binding energies of 2.7 kcal/mol were obtained for the (t) and (b) positions, while the binding energy of 2.6 kcal/mol for the hollow position (h) was slightly lower. While these values are already in very good agreement with the benchmark values, they were further improved upon by adding a fraction of the exact exchange; this made the hollow (h) position the preferred site for adsorption, as predicted by CCSD(T). The EE+vdW binding energies for the (t), (b) and (h) positions were 2.4, 2.3, and 2.5 kcal/mol, respectively. As was the case for the benzene−Au complex, these binding energies are slightly greater than the benchmark values. The spin moment remains constant at 1 μ_B for all internuclear distances, which is consistent with a negligible electrostatic interaction between the Ag atom and the carbon atoms of the benzene ring.

A different situation obtains for the benzene−Pd complex. Here, the covalent interaction between the metal and the arene means the binding energy is large; using the PBE method, it is predicted to be 26.3, 27.3, and 19.0 kcal/mol for the (t), (b), and (h) positions, respectively. These values are significantly higher than the benchmark CCSD(T) values. In contrast to the situation with the Ag complex, the inclusion of the vdW term substantially reduces the predicted binding energies. While this may be surprising at first sight, the kernel $\Phi(r, r')$ used to describe the interactions between electron densities (eq 1) becomes repulsive at small distances.[49] Thus, the PBE+vdW calculation corrects the overbinding predicted by PBE alone, giving binding energies of 21.5, 21.8, and 13.3 kcal/mol. It should be noted that such repulsive corrections are impossible in the various empirical DFT+D2 (or D3)[26] approaches, because D2 and D3 terms are always attractive, i.e., they provide a nonzero and positive (in terms of the definition of binding energy used in this paper) contribution to the binding energy. Incorporating a fraction of the exact exchange energy further reduced the calculated binding energy, as was the case for the benzene−Au complex. The EE+vdW binding energies for the (t), (b), and (h) positions were thus reduced to 17.2, 18.7, and 10.6 kcal/mol, respectively. As before, the inclusion of one-quarter of the exact exchange yielded DFT results that were very close to the benchmark value (although in this case, the DFT binding energies were slightly lower than the reference values), demonstrating that methods for improving on the treatment of long-range correlation effects (the vdW term) should be used in conjunction with methods that treat midrange exchange properly.

Graphene−M Complexes. The main advantage of calculations that use periodic plane-wave basis sets is that they can be applied to the study of extended systems. Our studies on benzene−M complexes demonstrated that the PBE functional can yield binding energies that agree very well with reference CCSD(T) values when augmented with a nonlocal vdW correction and one-quarter of the exact exchange (EE+vdW). We therefore used this method to obtain DFT benchmark energies for the interactions of metal atoms with a graphene sheet. In this context, it should be noted that PBE+vdW interaction energies for Cu, Ag, and Au atoms on graphene have been published very recently.[53] Our calculations differ from those reported in that publication, however, since (i) we included the contribution of the exact HF exchange in order to obtain more reliable interaction energies, and (ii) our calculations used carbon atoms that were fixed in place (i.e., no geometrical relaxation of the graphene sheet was allowed) in order to facilitate comparisons of the bonding of metals adsorbed on graphene with that in benzene and coronene complexes. The role of geometrical relaxation of the graphene surface is thoroughly discussed by Amft et al.[53]

Figures 14−16 and Table 4 summarize the calculated interaction energies for the graphene−M complexes. On examining the binding energy of the graphene−Au complex, it is apparent the bonding is dominated by vdW term, which stands in stark contrast to the situation in the benzene−Au complex. The binding energy calculated using the GGA/PBE approximation alone is very weak (∼1.6 kcal/mol), which is consistent with the GGA values of 2.2 kcal/mol for the most favorable (t) position reported in previous works.[12,13] The difference in the GGA binding energies can be attributed to the fact that in those previous works, the geometry of the graphene was allowed to

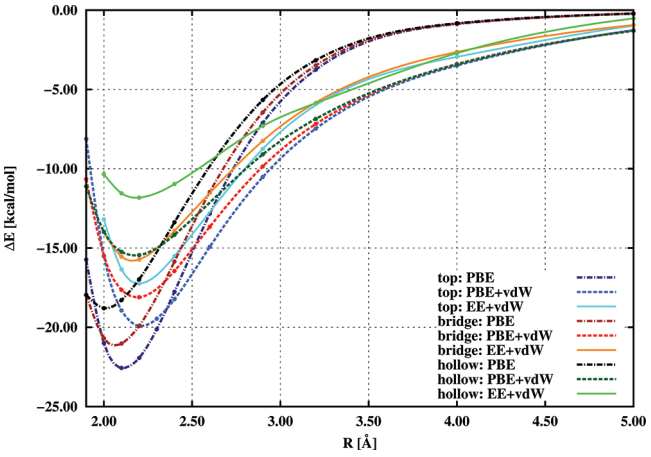

Figure 16. Periodic plane-wave DFT/PBE, DFT/PBE+vdW, and DFT/EE+vdW potential curves for the graphene−Pd complex with the metal adsorbed at the (t), (b), and (h) positions.

Table 4. Interaction Energies ΔE [kcal/mol] for Graphene−M (M = Ag, Au, Pd) Complexes with an Optimized Bond Length R [Å]

	graphene−Pd			graphene−Ag			graphene−Au		
	(t)	(b)	(h)	(t)	(b)	(h)	(t)	(b)	(h)
				PBE					
ΔE	−22.8	−21.3	−19.0	−0.6	−0.6	−0.6	−1.6	−1.6	−1.6
R	2.11	2.07	2.02	3.72	3.72	3.73	3.41	3.54	3.63
				PBE+vdW					
ΔE	−20.1	−18.3	−15.6	−4.3	−4.3	−4.2	−6.3	−6.4	−6.2
R	2.22	2.20	2.18	3.35	3.35	3.39	3.30	3.36	3.42
				EE+vdW					
ΔE	−17.4	−15.9	−12.0	−4.3	−4.3	−4.2	−5.6	−5.5	−5.2
R	2.21	2.17	2.18	3.35	3.35	3.39	3.14	3.07	3.33

relax (i.e., was optimized). It should also be noted that our test calculations using the B3LYP hybrid functional (data not shown) predicted no binding at all for gold in the (t) position on graphene, which would appear to support the hypothesis that gold binds only very weakly to graphene surfaces.

On the other hand, LDA calculations gave binding energies of 12.6, 12.2, and 10.3 kcal/mol for the (t), (b), and (h) positions, respectively (data not shown). These energies are twice as high as the benchmark values calculated for the coronene−Au complex, indicating unphysical overbinding by the LDA method; the electronic structures of coronene and graphite are certainly not sufficiently dissimilar to account for this discrepancy. These results clearly show that the LDA is inadequate for modeling the interactions of graphene with gold atoms or surfaces.

The PBE+vdW method gives rather uniform binding energies of 6.3, 6.4, and 6.2 kcal/mol for the (t), (b), and (h) positions, respectively. These values and the differences between them are in good agreement with the MP2 values calculated for the coronene−Au complex. In the original paper by Dion et al.[49] the authors suggested to replace the PBE exchange energy by its revPBE counterpart to obtain more accurate binding energies. We tested this scheme, which is becoming more and more popular, for the graphene−M (M = Pd, Au) complexes. The revPBE+vdW binding energies of 3.8, 3.9, and 3.9 kcal/mol for the (t), (b), and (h) positions in graphene−Au complex, respectively, are approximately two-times lower than the corresponding benchmark energies for coronene−Au complexes. The same applies also for graphene−Pd complexes (see the following paragraph). The small differences of the electronic structure between graphene and coronene, discussed in the previous paragraph, imply that the revPBE+vdW binding energies are significantly underestimated and that the revPBE+vdW method cannot be recommended for such type of calculations.

The carbon−metal bonding distances are longer than those in the benzene−Au complex because of the greater exchange repulsion between the Au atom and the carbon atoms in the graphene sheet. The elongation of bonding distances with respect to benzene complex is consistent with the elongation of the metal−carbon bond observed in the coronene−Au complex. As was the case with the benzene−M complexes, the incorporation of a fraction of the exact exchange energy slightly reduced the calculated binding energies. The EE+vdW binding energies for the (t), (b), and (h) positions were 5.6, 5.5, and 5.4 kcal/mol, respectively. It should be noted that the preferred (t) position of gold on graphene surface agrees with recent experimental data.[67] The incorporation of exact exchange reduces the distances between the metal atom and the graphene sheet, which are 3.14, 3.07, and 3.33 Å for the (t), (b), and (h) positions, respectively. The distance between the metal atom and the plane containing the arene increases consistently on going from benzene to coronene to graphene, and the calculated binding energies for the adsorption of gold atoms on graphene are somewhat lower than those for the coronene−Au complex. This is largely due to the underestimation of the charge-transfer contribution in the pure PBE GGA calculation, which is highlighted when one compares the results for the graphene and benzene complexes.

The energies of the graphene−Pd complex shown in Figure 16 continue the trend observed on going from benzene to coronene. The interaction energies for the top (t) and bond (b) positions are slightly lowered in comparison with benzene, whereas the energy of the hollow (h) site is higher. The PBE+vdW energies are 20.1, 18.3, and 15.6 kcal/mol and agree very well with those for the coronene−Pd complex. The only difference is that the (t) position is predicted to be the most stable for graphene, whereas the MP2 results for coronene predict that the above-bond position (b) is the most stable. The adsorption of Pd at the (b) position results in the formation of a partial covalent bond with neighboring carbon atoms, as was demonstrated by means of an overlap population analysis in the preceding section. The EE+vdW binding energies for the (t), (b), and (h) positions were 17.4, 15.9, and 12.0 kcal/mol, respectively. For the sake of completeness, the revPBE+vdW binding energies for the (t), (b), and (h) positions were 12.8, 10.9, and 8.2 kcal/mol, respectively.

Finally, examination of the energy profiles for the graphene−Ag complex reveals that silver atoms bind a little more strongly to graphene than to benzene, primarily because of stronger vdW (dispersion) interactions. In this case, the pure GGA predicts only very weak bonding of ∼0.6 kcal/mol, at large equilibrium distances of around 3.5 Å. Because of the interaction between the silver atom and the graphene sheet is dominated by dispersion forces, the energetic differences between the three adsorption sites examined were negligible. Adsorbed silver atoms can thus easily slide over a graphene surface; the barriers to their diffusion

relate primarily to the buckling of the graphene sheet, which is most pronounced at the hollow site.[53]

The interaction energies for the graphene−Ag complex calculated using the PBE+vdW method were 4.3, 4.3, and 4.2 kcal/mol for the (t), (b), and (h) positions, respectively. The vdW term is obviously dominant and is essential for accurately modeling the adsorption of Ag on graphene. Our results agree very well with PBE+vdW values published by Amft et al. (Ag: 4.5, 4.5, and 4.4 kcal/mol for the (t), (b), and (h) positions, respectively)[53] and also with the MP2 values calculated for the coronene−Ag complex. In accord with the negligible electrostatic interaction between silver and graphene, the inclusion of an exact exchange correction has little impact on the calculated interaction energies, changing them by less than 0.1 kcal/mol for all positions. As such, the PBE+vdW values can effectively be regarded as the benchmark in this case.

On comparing the results for coronene and graphene, it is apparent that MP2 and EE+vdW strongly favor the adsorption of Pd over Au or Ag. Moreover, these two methods both yield similar ratios for the binding energy of Pd relative to Au and Ag; the ratio for MP2 is 9:5:2, while that for EE+vdW is 9:3:2. The two methods also predict similar behavior for the binding energy on switching from benzene to coronene or graphene, in terms of both overall trends and absolute values.

5. CONCLUSIONS

WFT and DFT calculations performed for the benzene−M and coronene−M complexes (M = Ag, Au, Pd) indicate that Pd is bound most strongly, followed by Au and Ag. The difference in binding energy between the strongest and weakest complexes is, however, reduced on going from benzene to coronene. The nature of the adsorption of these three elements is different. While silver binds primarily via dispersion forces in both cases, the binding of gold is primarily attributable to charge-transfer interactions between the electron donor (benzene or coronene) and the electron acceptor (the gold atom). Relativistic effects are important in the binding of gold, and their neglect leads to dramatic underestimation of the binding energy. The binding of Pd is quite different again; it forms a (partial) covalent bond with the arene.

The CCSD(T) benchmark binding energies for the benzene−M (M = Pd, Au, Ag) complexes were 19.7, 4.2, 2.4 kcal/mol, respectively; the MP2 binding energies for the coronene−M (M = Pd, Au, Ag) complexes were 17.7, 7.0, 4.1 kcal/mol, respectively. These numbers indicate that the nature of the binding of the metal atoms does not change dramatically on going from benzene to coronene and that the values obtained at the benchmark CCSD(T) level can thus be used to characterize the adsorption of metals on a carbon surface.

Comparison between the reference CCSD(T) and plane-wave DFT calculations demonstrates that neither LDA nor GGA provide reliable binding energies. On the other hand, PBE+vdW performs well, but surprisingly, the revPBE+vdW underbinds studied complexes. The most accurate plane-wave DFT method identified was PBE+vdW with an exact exchange correction; referred here as EE+vdW. Using this method, the binding energies calculated for the benzene−M and graphene−M (M = Pd, Au, Ag) complexes were 18.7, 5.1, and 2.5 kcal/mol and 17.4, 5.6, and 4.3 kcal/mol, respectively. The values obtained for the benzene complexes agree with the benchmark CCSD(T) energies to within chemical accuracy (∼1 kcal/mol). Moreover, calculations using this method accurately reproduced the trends in binding energy observed on switching from benzene to coronene or graphene as well as the corresponding absolute reference values. By comparing the pure GGA binding energies to those calculated using the nonlocal vdW correlation, it was demonstrated that the vdW corrections are purely attractive only in Ag complexes; in Pd complexes, they are repulsive and serve to correct the overbinding predicted by the PBE method. This implies that using empirical corrections to simulate dispersion interactions can be counterproductive when studying graphene−metal systems, since corrections of this kind will always favor binding.

The good agreement obtained with two rather different computational methods (specifically, wave function-based CCSD(T) and MP2 with a local basis set and the density functional-based EE+vdW method, with a plane-wave basis set) indicates that the calculated graphene binding energies reported in this paper can be used as reliable benchmark values and that EE+vdW is a useful and practical method for accurate computational studies of extended systems. Moreover, it also demonstrates that coronene complexes are useful model systems for modeling adsorption on graphene with chemical accuracy.

AUTHOR INFORMATION

Corresponding Author

*E-mail: michal.otyepka@upol.cz; pavel.hobza@uochb.cas.cz.

Author Contributions

‖These authors contributed equally to this work.

ACKNOWLEDGMENT

This work was a part of research project no. Z40550506 of the Institute of Organic Chemistry and Biochemistry, Academy of Sciences of the Czech Republic. It was also supported by the Korea Science and Engineering Foundation (World Class University program R32-2008-000-10180-0), by grants no. LC512 and MSM6198959216 from the Ministry of Education, Youth and Sports of the Czech Republic and by grant No. P208/10/1742 from the Grant Agency of the Czech Republic. It was also supported by the operational program Research and Development for Innovations of European Regional Development Fund (CZ.1.05/2.1.00/03.0058) and the Operational Program Education for Competitiveness of European Social Fund (CZ.1.07/2.3.00/20.0017). The support of Praemium Academiae, Academy of Sciences of the Czech Republic, awarded to P.H. in 2007 is also acknowledged.

REFERENCES

(1) Sundaram, R. S.; Steiner, M.; Chiu, H.-Y.; Engel, M.; Bol, A. A.; Krupke, R.; Burghard, M.; Kern, K.; Avouris, P. *Nano Lett.* **2011**, *11*, 3833.

(2) Baby, T. T.; Aravind, S. S. J.; Arockiadoss, T.; Rakhi, R. B.; Ramaprabhu, S. *Sens. Actuators, B* **2010**, *145*, 71.

(3) Hong, W. J.; Bai, H.; Xu, Y. X.; Yao, Z. Y.; Gu, Z. Z.; Shi, G. Q. *J. Phys. Chem. C* **2010**, *114*, 1822.

(4) Li, Y.; Fan, X. B.; Qi, J. J.; Ji, J. Y.; Wang, S. L.; Zhang, G. L.; Zhang, F. B. *Mater. Res. Bull.* **2010**, *45*, 1413.

(5) Li, Y.; Fan, X. B.; Qi, J. J.; Ji, J. Y.; Wang, S. L.; Zhang, G. L.; Zhang, F. B. *Nano Res.* **2010**, 3, 429.

(6) Scheuermann, G. M.; Rumi, L.; Steurer, P.; Bannwarth, W.; Mülhaupt, R. *J. Am. Chem. Soc.* **2009**, *131*, 8262.

(7) Shan, C. S.; Yang, H. F.; Han, D. X.; Zhang, Q. X.; Ivaska, A.; Niu, L. *Biosens. Bioelectron.* **2010**, *25*, 1070.
(8) Xiong, Z. G.; Zhang, L. L.; Ma, J. Z.; Zhao, X. S. *Chem. Commun.* **2010**, *46*, 6099.
(9) Jensen, P.; Blase, X.; Ordejón, P. *Surf. Sci.* **2004**, *564*, 173.
(10) Wang, G. M.; BelBruno, J. J.; Kenny, S. D.; Smith, R. *Phys. Rev. B* **2004**, *69*, 195412.
(11) Akola, J.; Häkkinen, H. *Phys. Rev. B* **2006**, *74*, 165404.
(12) Amft, M.; Sanyal, B.; Eriksson, O.; Skorodumova, N. V. *J. Phys.: Condens. Matter* **2011**, *23*, 205301.
(13) Chan, K. T.; Neaton, J. B.; Cohen, M. L. *Phys. Rev. B* **2008**, *77*, 235430.
(14) Jalkanen, J. P.; Halonen, M.; Fernandez-Torre, D.; Laasonen, K.; Halonen, L. *J. Phys. Chem. A* **2007**, *111*, 12317.
(15) Varns, R.; Strange, P. *J. Phys.: Condens. Matter* **2008**, *20*, 225005.
(16) Arthur, J. R.; Cho, A. Y. *Surf. Sci.* **1973**, *36*, 641.
(17) Da Silva, A. J. R.; Carrijo-Faria, J.; da Silva, E. Z.; Fazzio, A. *Nanotechnology* **2003** *vol 3*, 2003.
(18) Wang, G. M.; BelBruno, J. J.; Kenny, S. D.; Smith, R. *Surf. Sci.* **2003**, *541*, 91.
(19) Yagi, Y.; Briere, T. M.; Sluiter, M. H. F.; Kumar, V.; Farajian, A. A.; Kawazoe, Y. *Phys. Rev. B* **2004**, *69*, 075414.
(20) López-Corral, I.; Germán, E.; Juan, A.; Volpe, M. A.; Brizuela, G. P. *J. Phys. Chem. C* **2011**, *115*, 4315.
(21) Riley, K. E.; Pitoňák, M.; Jurečka, P.; Hobza, P. *Chem. Rev.* **2010**, *110*, 5023.
(22) Neogrády, P.; Urban, M. *Int. J. Quantum Chem.* **1995**, *55*, 187.
(23) Neogrády, P.; Urban, M.; Hubač, I. In *Recent Advances in Coupled-Cluster Methods*; Bartlett, R. J., Ed.; World Scientific: Singapore, 1997, p 275.
(24) Watts, J. D.; Gauss, J.; Bartlett, R. J. *J. Chem. Phys.* **1993**, *98*, 8718.
(25) Møller, C.; Plesset, M. S. *Phys. Rev.* **1934**, *46*, 0618.
(26) Grimme, S.; Antony, J.; Ehrlich, S.; Krieg, H. *J. Chem. Phys.* **2010**, *132*, 154104.
(27) Zhao, Y.; Truhlar, D. G. *J. Chem. Phys.* **2006**, *125*, 194101.
(28) Zhao, Y.; Truhlar, D. G. *J. Chem. Theory Comput.* **2007**, *3*, 289.
(29) Zhao, Y.; Truhlar, D. G. *Theor. Chem. Acc.* **2008**, *120*, 215.
(30) Heckert, M.; Heun, O.; Gauss, J.; Szalay, P. G. *J. Chem. Phys.* **2006**, *124*, 124105.
(31) Iliaš, M.; Kellö, V.; Urban, M. *Acta Phys. Slovaca* **2010**, *60*, 259.
(32) Douglas, M.; Kroll, N. M. *Ann. Phys.* **1974**, *82*, 89.
(33) Hess, B. A.; Chandra, P. *Phys. Scr.* **1987**, *36*, 412.
(34) Roos, B. O.; Lindh, R.; Malmqvist, P. A.; Veryazov, V.; Widmark, P. O. *J. Phys. Chem. A* **2004**, *108*, 2851.
(35) Roos, B. O.; Lindh, R.; Malmqvist, P. A.; Veryazov, V.; Widmark, P. O. *J. Phys. Chem. A* **2005**, *109*, 6575.
(36) Kellö, V.; Sadlej, A. J. *Theor. Chim. Acta* **1996**, *94*, 93.
(37) Sadlej, A. J. *Collect. Czech. Chem. Commun.* **1988**, *53*, 1995.
(38) VanLenthe, J. H.; VanDuijneveldt-van de Rijdt, J. G. C. M.; VanDuijneveldt, F. B. *Adv. Chem. Phys.* **1987**, *69*, 521.
(39) Antušek, A.; Urban, M.; Sadlej, A. J. *J. Chem. Phys.* **2003**, *119*, 7247.
(40) Granatier, J.; Urban, M.; Sadlej, A. *J. J. Phys. Chem. A* **2007**, *111*, 13238.
(41) Granatier, J.; Urban, M.; Sadlej, A. J. *Chem. Phys. Lett.* **2010**, *484*, 154.
(42) Boys, S. F.; Bernardi, F. *Mol. Phys.* **1970**, *19*, 553.
(43) Karlström, G.; Lindh, R.; Malmqvist, P. A.; Roos, B. O.; Ryde, U.; Veryazov, V.; Widmark, P. O.; Cossi, M.; Schimmelpfennig, B.; Neogrády, P.; Seijo, L. *Comput. Mater. Sci.* **2003**, *28*, 222.
(44) Ahlrichs, R.; Bär, M.; Häser, M.; Horn, H.; Kölmel, C. *Chem. Phys. Lett.* **1989**, *162*, 165.
(45) Frisch, M. J.; Trucks, G. W.; Schlegel, H. B.; Scuseria, G. E.; Robb, M. A.; Cheeseman, J. R.; Scalmani, G.; Barone, V.; Mennucci, B.; Petersson, G. A.; Nakatsuji, H.; Caricato, M.; Li, X.; Hratchian, H. P.; Izmaylov, A. F.; Bloino, J.; Zheng, G.; Sonnenberg, J. L.; Hada, M.; Ehara, M.; Toyota, K.; Fukuda, R.; Hasegawa, J.; Ishida, M.; Nakajima, T.; Honda, Y.; Kitao, O.; Nakai, H.; Vreven, T.; Montgomery, J. A., Jr.; Peralta, J. E.; Ogliaro, F.; Bearpark, M.; Heyd, J. J.; Brothers, E.; Kudin, K. N.; Staroverov, V. N.; Kobayashi, R.; Normand, J.; Raghavachari, K.; Rendell, A.; Burant, J. C.; Iyengar, S. S.; Tomasi, J.; Cossi, M.; Rega, N.; Millam, N. J.; Klene, M.; Knox, J. E.; Cross, J. B.; Bakken, V.; Adamo, C.; Jaramillo, J.; Gomperts, R.; Stratmann, R. E.; Yazyev, O.; Austin, A. J.; Cammi, R.; Pomelli, C.; Ochterski, J. W.; Martin, R. L.; Morokuma, K.; Zakrzewski, V. G.; Voth, G. A.; Salvador, P.; Dannenberg, J. J.; Dapprich, S.; Daniels, A. D.; Farkas, Ö.; Foresman, J. B.; Ortiz, J. V.; Cioslowski, J.; Fox, D. J. *Gaussian 09*, revision A.02; Gaussian, Inc.: Wallingford, CT, 2009.
(46) Blöchl, P. E. *Phys. Rev. B* **1994**, *50*, 17953.
(47) Kresse, G.; Joubert, D. *Phys. Rev. B* **1999**, *59*, 1758.
(48) Perdew, J. P.; Burke, K.; Ernzerhof, M. *Phys. Rev. Lett.* **1996**, *77*, 3865.
(49) Dion, M.; Rydberg, H.; Schröder, E.; Langreth, D. C.; Lundqvist, B. I. *Phys. Rev. Lett.* **2005**, *95*, 109902.
(50) Lazić, P.; Atodiresei, N.; Alaei, M.; Caciuc, V.; Blügel, S.; Brako, R. *Comput. Phys. Commun.* **2010**, *181*, 371.
(51) Klimeš, J.; Bowler, D. R.; Michaelides, A. *J. Phys.: Condens. Matter* **2010**, *22*, 022201 and references therein.
(52) BelBruno, J. J. *Surf. Sci.* **2005**, *577*, 167.
(53) Amft, M.; Lebègue, S.; Eriksson, O.; Skorodumova, N. V. *J. Phys.: Condens. Matter* **2011**, *23*, 395001.
(54) Peterson, K. A.; Puzzarini, C. *Theor. Chem. Acc.* **2005**, *114*, 283.
(55) Peterson, K. A.; Figgen, D.; Dolg, M.; Stoll, H. *J. Chem. Phys.* **2007**, *126*, 124101.
(56) Ishikawa, T. *Jpn. J. Appl. Phys.* **1993**, *32*, 4779.
(57) Scheer, M.; Brodie, C. A.; Bilodeau, R. C.; Haugen, H. K. *Phys. Rev. A* **1998**, *58*, 2051.
(58) Neogrády, P.; Kellö, V.; Urban, M.; Sadlej, A. J. *Int. J. Quantum Chem.* **1997**, *63*, 557.
(59) Loock, H. P.; Beaty, L. M.; Simard, B. *Phys. Rev. A* **1999**, *59*, 873.
(60) Bilodeau, R. C.; Scheer, M.; Haugen, H. K. *J. Phys. B: At. Mol. Opt. Phys.* **1998**, *31*, 3885.
(61) Brown, C. M.; Ginter, M. L. *J. Opt. Soc. Am.* **1978**, *68*, 243.
(62) Hotop, H.; Lineberger, W. C. *J. Phys. Chem. Ref. Data* **1985**, *14*, 731.
(63) Lee, K.; Murray, E. D.; Kong, L.; Lundqvist, B. I.; Langreth, D. C. *Phys. Rev. B* **2010**, *82*, 081101.
(64) Dargel, T. K.; Hertwig, R. H.; Koch, W. *Mol. Phys.* **1996**, *96*, 583.
(65) Yi, H.-B.; Lee, H. M.; Kim, K. S. *J. Chem. Theory Comput.* **2009**, *5*, 1709.
(66) Yi, H.-B.; Diefenbach, M.; Choi, Y. C.; Lee, E. C.; Lee, H. M.; Hong, B. H.; Kim, K. S. *Chem.—Eur. J.* **2006**, *12*, 4885.
(67) Zan, R.; Bangert, U.; Ramasse, Q.; Novoselov, K. S. *Nano Lett.* **2011**, *11*, 1087.